ACS Chemical Neuroscience

Research Article

pubs.acs.org/chemneuro

A Novel Restricted Diffusion Model of Evoked Dopamine

Seth H. Walters, I. Mitch Taylor, Zhan Shu, and Adrian C. Michael*

Department of Chemistry, University of Pittsburgh, Pittsburgh, Pennsylvania 15260, United States

Supporting Information

ABSTRACT: In vivo fast-scan cyclic voltammetry provides high-fidelity recordings of electrically evoked dopamine release in the rat striatum. The evoked responses are suitable targets for numerical modeling because the frequency and duration of the stimulus are exactly known. Responses recorded in the dorsal and ventral striatum of the rat do not bear out the predictions of a numerical model that assumes the presence of a diffusion gap interposed between the recording electrode and nearby dopamine terminals. Recent findings, however, suggest that dopamine may be subject to restricted diffusion processes in brain extracellular space. A numerical model cast to account for restricted diffusion produces excellent agreement between simulated and observed responses recorded under a broad range of anatomical, stimulus, and pharmacological conditions. The numerical model requires four, and in some cases only three, adjustable parameters and produces meaningful kinetic parameter values.

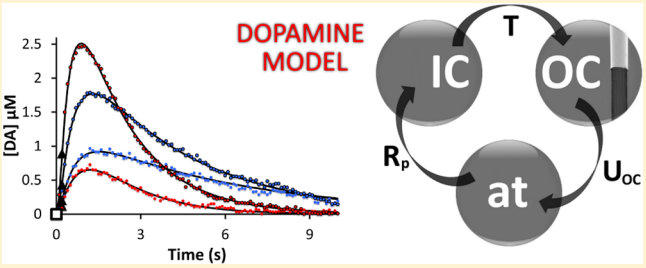

KEYWORDS: *Model, dopamine, restricted diffusion, voltammetry, diffusion, domain*

Dopamine (DA) is a neurotransmitter that contributes significantly to normal brain function[1] and is implicated in multiple neurological and psychiatric disorders.[2−4] So, it is highly significant to understand the processes by which DA molecules convey information from DA terminals to pre- and postsynaptic DA receptors.[5] Those processes include DA release,[6] reuptake,[7] metabolism,[8] and mass transport.[9] Insight into these processes can be gained by recording DA with in vivo fast-scan cyclic voltammetry (FSCV) at implantable, DA-sensitive, DA-selective carbon fiber microelectrodes.[10]

In vivo FSCV is used frequently to record electrically evoked DA overflow.[11−15] The evoked responses are suitable targets for mathematical modeling because the timing, frequency, and duration of the stimulus are exactly known. Mathematical modeling provides quantitative insight into the kinetic and mass transport parameters that govern DA's extracellular dynamics. Equation 1 is a starting point for mathematical modeling

$$\frac{d[DA]}{dt} = [DA]_p f - \frac{V_{max}[DA]}{[DA] + K_M} \quad (1)$$

where [DA] is the evoked extracellular DA concentration, $[DA]_p$ is the concentration of DA released per electrical stimulus pulse, f is the stimulus frequency, and V_{max} and K_M are the maximal rate and Michaelis constant, respectively, of DA uptake.[16] According to eq 1, the evoked DA overflow reflects a balance between the rates of evoked DA release ($[DA]_p f$) and Michaelis−Menten DA uptake ($(V_{max}[DA])/([DA] + K_M)$). Equation 1 predicts that the DA concentration should rise during the stimulus and decay thereafter (Figure 1a). However, experimental responses often exhibit additional features,[18−23] known as lag, overshoot, and hang-up (Figure 1a), that are not captured by eq 1 alone.

SHORTCOMINGS OF THE DIFFUSION GAP (DG) MODEL

The DA model most widely used to date postulates that the DA concentration observed by FSCV is governed by eq 1 but is also affected by diffusional distortion due to a physical gap interposed between the electrode and nearby DA terminals.[16] Accordingly, lag and overshoot are postulated to be experimental errors stemming from a poor choice of recording site.[17] Consequently, optimization of the placement of FSCV electrodes near putative DA "hot spots" has been advocated as a procedure to minimize the perceived errors associated with diffusional distortion.[17]

However, the diffusion gap (DG) model makes very specific predictions about lag and overshoot that are not borne out by observations. If the gap were a physical space, then it should always cause lag and overshoot together and the lag and overshoot duration should always be of similar magnitude. In addition, lag and overshoot should not vary with the stimulus or pharmacological conditions. Moreover, there is no obvious reason that a diffusion gap should cause hang-up. However, evoked responses with lag but without overshoot, with overshoot but without lag, with lag and overshoot that vary with stimulus and pharmacological conditions, and with hang-

Received: March 25, 2014
Revised: June 26, 2014
Published: July 1, 2014

   dx.doi.org/10.1021/cn5000666 | ACS Chem. Neurosci. 2014, 5, 776−783

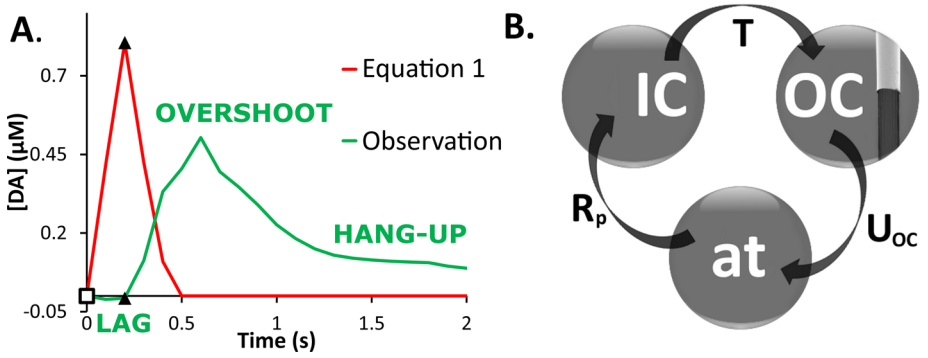

Figure 1. (A) Evoked responses, as predicted by eq 1 (red line), rise during the stimulus and decay back to zero after the stimulus ends. However, observed responses (green line) also exhibit lag (an initial delay in the appearance of the signal), overshoot (the signal continues to rise after the stimulus ends), and hang-up (the signal remains elevated for prolonged periods after the stimulus ends instead of returning to baseline). The open square indicates the start of the stimulus, and the closed triangles indicate the end of the stimulus. (B) Schematic representation of the RD model (see the Methods section for definitions of the parameters). The extracellular space is divided into inner (IC) and outer (OC) compartments. DA is released from axon terminals (at) to the IC, is subsequently transported to the OC, and is removed from the OC by uptake. The model postulates that FSCV recording takes place in the OC.

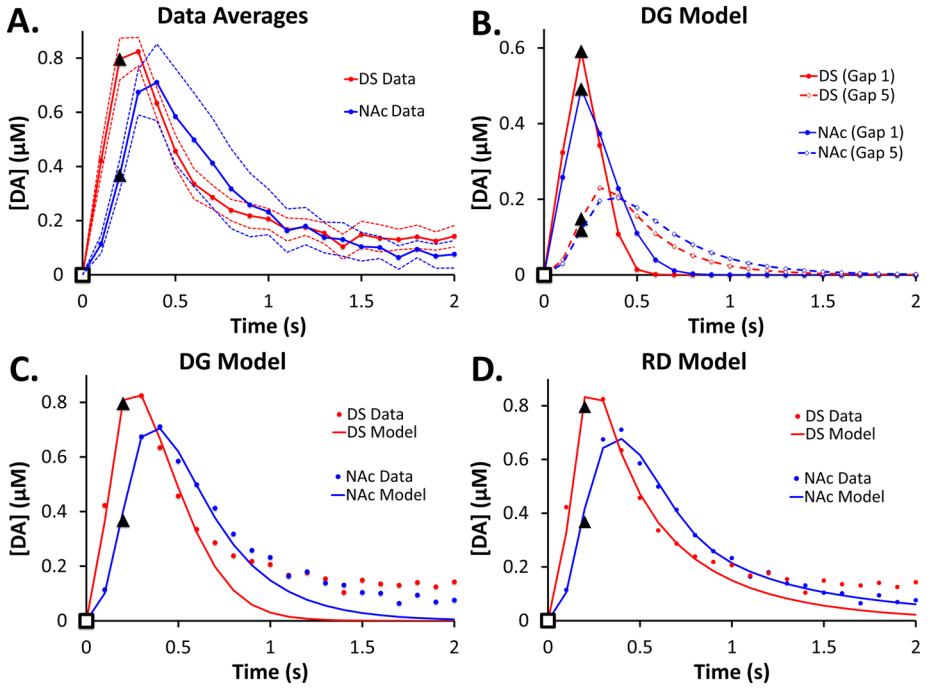

Figure 2. (A) Evoked responses recorded in fast domains of the DS and NAc (stimulus = 200 ms, 60 Hz, 250 μA): the solid lines are the averaged responses, and the dotted lines are the SEM intervals. (B) DG simulations using region-specific parameter values and *Gap* values of 1 and 5. (C) DG simulations of the averaged DS and NAc data points (SEMs omitted for clarity). (D) RD simulations of the averaged DS and NAc data points (SEMs omitted for clarity). The open square indicates when the stimulus begins, and the closed triangle marks the data point at the end of the stimulus. The parameter values are reported in the Supporting Information.

up are absolutely commonplace.[18−20] Hence, there exists an urgent need for a new model.

INTRODUCTION OF THE RESTRICTED DIFFUSION (RD) MODEL

Recent findings from our laboratory[18−23] led us to hypothesize that DA molecules are subjected to restricted diffusion mechanisms that inhibit their ability to diffuse freely through the extracellular space. Restricted diffusion might, for example, play an important role in maintaining the distinctions between the fast and slow DA domains that we have documented in the dorsal striatum (DS) and nucleus accumbens (NAc). Nicholson and others have identified several potential mechanisms of restricted diffusion, including the trapping of molecules in dead space microdomains,[24] the obstruction of passageways by macromolecules,[25,26] and the presence of either specific[9] or nonspecific[27] binding sites that impede the diffusing molecule.

Our objective is to introduce a new DA model to investigate whether a generic restricted diffusion mechanism offers a plausible explanation for the lag, overshoot, and hang-up features of evoked DA responses. Conceptually, restricted diffusion introduces a delay, or pause, in the transport of DA from its release sites to the FSCV electrode. To cast a mathematical model of such a delay, we divided the extracellular space into an inner and outer compartment (IC and OC, respectively, Figure 1B). The model postulates that

dx.doi.org/10.1021/cn5000666 | ACS Chem. Neurosci. 2014, 5, 776−783

DA is released into and temporarily held in the inner compartment, that DA is detected after it undergoes transport to the outer compartment, and that the time DA spends trapped in the inner compartment represents the restriction of its diffusion in the extracellular space.

From a modeling perspective, the compartments function akin to an equivalent circuit diagram that simplifies the analysis of a complex electronic circuit. However, several possibilities also present themselves as physical compartments in brain extracellular space. Hypothetically, the synaptic cleft or the perisynaptic space, which is sometimes encased by a sheath of glial processes, might constitute physical compartments. Alternately, the compartments might represent the dead spaces, blocked passages, or binding sites identified by Nicholson and co-workers.[24−27]

The restricted diffusion (RD) model postulates that DA (1) is released initially to the inner compartment, (2) is subsequently transported to the outer compartment, (3) is detected by FSCV in the outer compartment, and (4) is cleared from the outer compartment by DA uptake (Figure 1B). For clarity, we state that the model does not postulate DA uptake from the inner compartment. This might imply that uptake from the inner compartment does not occur, which might be the case if the inner compartment represents binding sites or dead spaces. Alternately, uptake from the inner compartment might prevent some of the released DA from reaching the FSCV electrode, which would render uptake from the inner compartment invisible to FSCV.

The principal justification for these postulates is that the resulting RD model reproduces the lag, overshoot, and hang-up features of numerous evoked DA responses recorded under a broad range of conditions (vide infra). This is accomplished with only four, and in some cases only three, adjustable parameters.

RESULTS AND DISCUSSION

We first present the models and their fits to various data sets (simulated data points are reported at 100 ms intervals to match the FSCV recordings) and subsequently discuss the parameter values. The parameter values are tabulated in two formats in the Supporting Information. In the first format, the parameters are indexed to the figures presented below. In the second format, the parameters are listed according to brain region, domain, stimulus duration, and drug treatment.

RESPONSE FEATURES UNIQUE TO THE DS AND NAC

Evoked responses recorded in the fast domains of the DS and NAc exhibit marked distinctions in amplitude and profile (Figure 2A; the symbols and solid lines are the averaged evoked responses, and the dotted lines show the SEM interval (n = 16 DS; n = 7 NAc); stimulus = 60 Hz, 200 ms, 250 μA; data are from refs 19 and 20). Lag and overshoot are far more pronounced in the NAc, and the signal decay after the peak is slower in the NAc. The distinctions between the DS and NAc responses are well-known in the literature.[20,33,34]

We performed DG simulations using the DS- and NAc-specific kinetic parameters reported by Wu et al.,[35] who attributed diffusional distortion of the responses to a film on the electrode. Because there is no obvious reason that the thickness of a film on the electrode should depend on the brain region in which the electrode is placed, we ran DS and NAc simulations with identical gap values (Figure 2B reports pairs of simulations with *Gap* = 1 and with *Gap* = 5; the *Gap* parameter is defined in the Methods section). However, when the same *Gap* value is used, the simulations do not reproduce the distinct lag and overshoot features of the DS and NAc responses.

The DG model produces different lag and overshoot features only when different *Gap* values are used (Figure 2c; simulations using *Gap* = 1 for the DS and *Gap* = 5 for the NAc). The improved fit, however, carries with it the surprising implication that the gap width is a property of the brain region, not just a film on the electrode. The simulations still do not capture the hang-up feature; as mentioned above, a diffusion gap is not expected to produce a hang-up.

We find the implication (Figure 2c) that the gap is a property of the brain region to be highly confusing. According to the DG model, the gap is between the electrode and the active tissue zone. So, the implication of Figure 2c is that the electrodes are closer to DA terminals of the DS than the NAc: we know of no reason why this should be so. Studies show a difference in the spacing between DA terminals of the DS and NAc.[33] A difference in the spacing might affect DA_p and V_{max}, because these are spatially averaged quantities. However, the values of DA_p and V_{max} do not affect lag and overshoot (Figure 2b): only the width of the gap does that. According to the DG model, a difference in the spacing of the terminals would affect the response amplitude but not the lag and overshoot. So, there is no obvious reason that the gap should be brain region specific.

Figure 2c also illustrates the impact of the lag and overshoot on the quantification of DA's kinetic parameters. Whereas prior reports suggest that DA release and uptake are faster in the DS,[35] the simulations in Figure 2C indicate that DA release (DA_p) and DA clearance (V_{max}) are faster in the NAc. Thus, correctly accounting for lag and overshoot has significant bearing on the kinetic analysis.

During this work, we did not apply either the convolution or deconvolution algorithms used in prior studies to account for diffusional distortions of evoked DA responses.[17,35,36] Unless extreme caution is used, it appears possible that these algorithms can accidently distort response features not caused by diffusion across a gap, including lag and overshoot, and thereby confound the quantification of DA's kinetic parameters. During this work, we simulate only the "raw" data, without using convolution, deconvolution, or principal component algorithms.

The RD simulations produce improved overall fits to the observed DS and NAc responses (Figure 2D). The parameters for curve fitting were identified objectively with the search algorithm. There has been some controversy over the source of the hang-up,[37,38] so here we included only data points between 0 and 1 s in the parameter search because these data points are confirmed to be due to DA by their background-subtracted voltammograms. Even so, the RD simulations provide good fits to the rising phase of the evoked responses and an improved fit to the hang-up, especially in the case of the NAc.

DS FAST AND SLOW DOMAINS

We ran DG simulations of fast and slow DS responses (Figure 3; symbols are averages, and SEMs are omitted for clarity; stimulus = 60 Hz, 1 s, 250 μA). We fixed K_M at 0.2 μM, a value cited many times in the literature.[39] A *Gap* of 2 reproduces the minimal lag and overshoot of the fast response (Figure 3a, red), but, overall, the fit is poor. A *Gap* of 10 reproduces the prominent lag in the slow response (Figure 3a, blue), but,

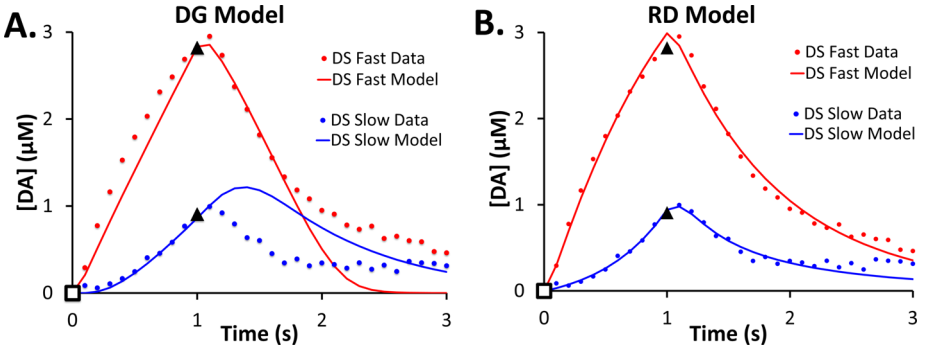

Figure 3. Fits of the DG (A) and RD (B) models to averaged responses from fast and slow domains of the dorsal striatum. The parameter values for these fits are reported in the Supporting Information.

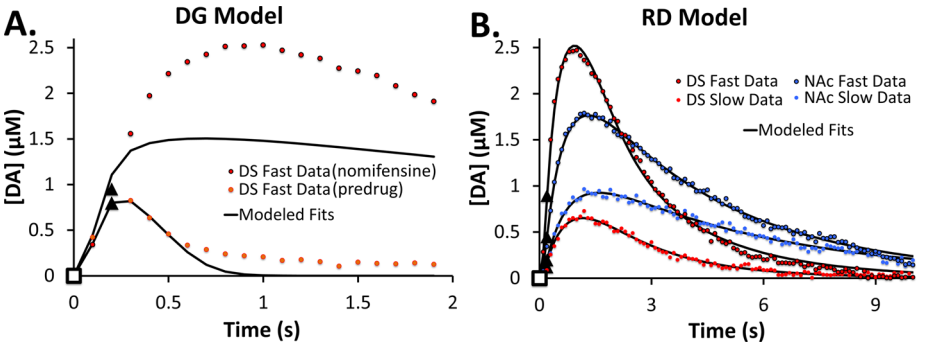

Figure 4. Fits of the DG (A) and RD (B) models to averaged responses from the dorsal striatum (A, B) and nucleus accumbens (B). In panel A, "predrug" refers to the stimulus as collected at a recording site in a drug naive rat, whereas "nomifensine" refers to data collected at the same site after i.p. administration of the competitive uptake inhibitor nomifensine. The parameter values are reported in the Supporting Information.

overall, the fit is poor. The DG model cannot produce responses with a prominent lag but no overshoot even though such responses are commonplace in slow domains.[18,19] The RD model produces better fits to the fast and slow DS responses (Figure 3B).

EFFECTS OF NOMIFENSINE, A COMPETITIVE DAT INHIBITOR

Prior studies based on the DG model have concluded that nomifensine acts solely by increasing the K_M of DA uptake.[40] However, in fast domains, nomifensine dramatically increases the duration and amplitude of overshoot even though the responses exhibit no lag (Figure 4A; the symbols are the averaged responses, and SEMs are omitted for clarity; stimulus = 60 Hz, 200 ms, 250 μA; data are from ref 19). DG simulations fail to reproduce this feature (Figure 4A, lines) even when K_M is increased to 20 μM, which produces a maximum effect.

In animals treated with nomifensine, evoked responses with prominent overshoot and no lag are absolutely commonplace.[13,18−20] As we have documented before,[21] DG simulations do not reproduce overshoot without lag, so we conclude that the DG model does not capture the key features of postnomifensine responses. Wightman and co-workers also encountered difficulty fitting the original DG model to postnomifensine responses and introduced a revised model.[28] However, the premise of the revised model, that nomifensine increases the apparent gap width, is inconsistent with nomifensine's ability to decrease lag (i.e., decrease the gap) in slow domains of the DS and NAc.[18−20] Thus, the revised DG model does not offer a comprehensive explanation of nomifensine's actions.

The RD model, using only four adjustable parameters (see also Figure 6, below), produces excellent fits to postnomifensine responses from the fast and slow domains of the DS and NAc (Figure 4B; symbols are average responses, and SEMs are omitted for clarity; stimulus = 60 Hz, 200 ms, 250 μA; data are from refs 19 and 32). Thus, the RD model captures evoked responses with prominent overshoot but no lag. The RD model produces excellent fits to these postnomifensine responses out to 10 s, i.e., including the hang-up: all of these data points are identifiable as DA from their background-subtracted cyclic voltammograms.

We ran RD simulations of pre- (Figure 5, blue) and postnomifensine (Figure 5, green) responses from the fast and slow domains of the DS and NAc (Figure 5; the simulations are shown as lines, the averaged data points are shown as symbols, and SEMs are omitted for clarity; stimulus = 60 Hz for 0.2, 1, and 3 s, 250 μA; data are from refs 19, 20, and 32). We used the search algorithm to identify all of the parameters. The RD model provides excellent fits to the data, with a few exceptions, so we conclude that the RD model captures most, but not quite all, of the features of these evoked responses.

PARAMETER VALUES

We used the search algorithm to quantify the parameters used in the RD simulations of Figures 2−5. We have imposed no constraints on any parameters values, and we have not employed any convolution, deconvolution, or principal components methods. We believe this to be an objective approach to quantifying the parameters.

dx.doi.org/10.1021/cn5000666 | ACS Chem. Neurosci. 2014, 5, 776−783

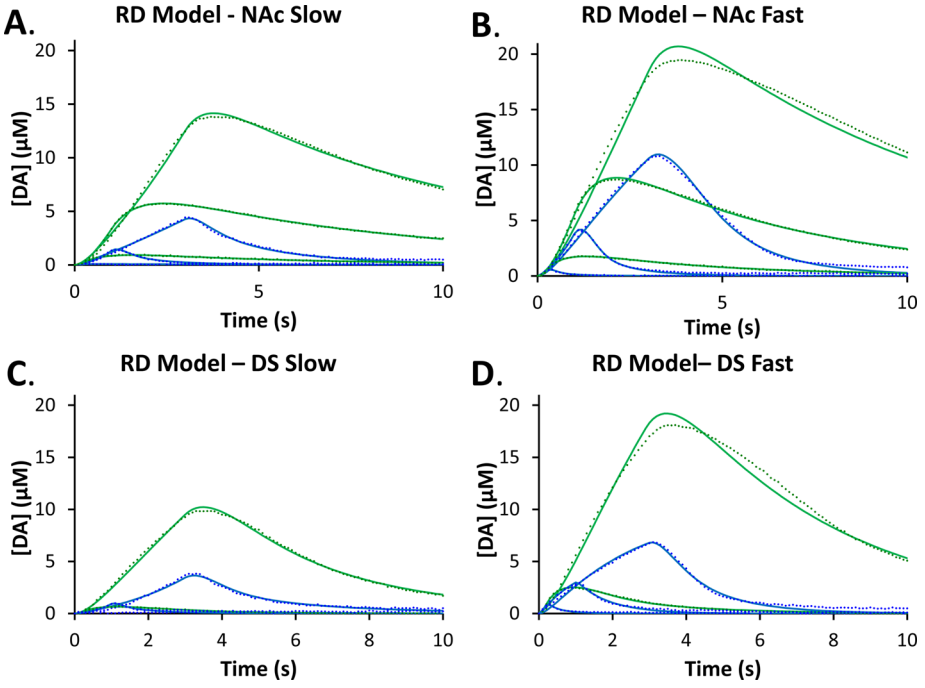

Figure 5. Fits of the RD model to averaged responses from the nucleus accumbens (A, B) and dorsal striatum (C, D) both before (blue) and after (green) animals were treated with nomifensine. The parameter values are listed in the Supporting Information.

The RD model produced some extreme parameter values (Supporting Information). The V_{max} values reach as high as 910 and 3200 μM s^{-1} in some cases. However, these extreme V_{max} values are paired with equally extreme K_M values of 41.4 and 1600 μM, respectively. Inspection of the data shows that the search algorithm produces these extreme values when the clearance profiles exhibit first-order behavior. Then, the algorithm optimizes the pseudo-first-order rate constants ($k = V_{max}/K_M$), which have perfectly reasonable values of 22 s^{-1} (from animals not treated with nomifensine) and 2 s^{-1} (from animals treated with nomifensine).

It is important to emphasize that in instances where clearance profile exhibits first-order behavior the data contain no intrinsic information about V_{max} or K_M. For this reason, we have included the pseudo-first-order rate constants in the parameter tables in the Supporting Information.

Unexpectedly, the parameters obtained with the RD model vary consistently with the stimulus duration (Supporting Information). For reasons we do not yet understand, the DA release (R_p), clearance (k), and transport (T) parameters decreased (with one or two exceptions) as the stimulus duration increased. We speculate that time-dependent factors such as depletion of the readily releasable pool, depletion of the DA terminals' energy reserves, or changes in the occupation of DA autoreceptors might be contributing factors. Such factors are not yet built into the RD model and might be targets for future refinements of the model.

Because of the variation of the parameters with the stimulus duration, the remainder of this discussion focuses on simulations of the briefest available responses. This decision rests on the idea that time-dependent factors should have minimum impact when the stimulus is brief. Table 1 lists the parameters obtained from simulations of responses to brief stimuli in the DS and NAc recorded before (0.2 s duration in fast domains and 1 s duration in slow domains) and after (0.2 s duration) animals were treated with nomifensine.

Table 1. Parameters Obtained by RD Simulations of the Response to Brief Stimuli

	R_p (mols × 10^{21})	V_{max} (μM/s)	T (s^{-1})	K_M (μM)	k (s^{-1})
DS fast, 0.2 s	39	106	1.77	1.88	56.2
DS slow, 1 s	25	54.7	0.51	0.65	84.2
NAc fast, 0.2 s	45	23.1	0.62	0.25	92.5
NAc slow, 1 s	17	36.4	0.50	0.84	43.3
DS fast, 0.2 s + nomi	47	20.2	0.34	3.36	6.0
DS slow, 0.2 s + nomi	5.6	7.7	0.45	3.67	2.1
NAc fast, 0.2 s + nomi	29	29.6	0.23	12.3	2.4
NAc slow, 0.2 s + nomi	16	16.5	0.18	8.6	1.9

The parameters values in Table 1 exhibit good agreement with several expectations. DA release and clearance are inherently faster in the NAc fast domains than the DS fast domains: this confirms the finding of Figure 2C. DA release and V_{max} are larger in the DS fast domains than the DS slow domains, as previously reported.[21] Likewise, R_p and k are higher in the NAc fast domains than the NAc slow domains.[32] Nomifensine dramatically slowed the kinetics of DA clearance (we do not discuss here the postnomifensine K_M and V_{max} values; see Figure 6).

However, the RD simulations do not confirm prior reports that nomifensine acts solely by changing the K_M of uptake, even though nomifensine is primarily a competitive uptake inhibitor. In all but the DS fast domain, nomifensine also slowed DA release. This might reflect nomifensine's secondary actions as an indirect D2 agonist.[21,41,42] Moreover, the absence of this effect in the DS fast domain is consistent with our finding that

dx.doi.org/10.1021/cn5000666 | ACS Chem. Neurosci. 2014, 5, 776−783

DS fast domain is insensitive to the D2 antagonist, raclopride.[21] Nomifensine also decreased the transport parameter, which might be a consequence of the accumulation of DA in the outer compartment.

Because, as mentioned above, the simulations found instances of first-order DA clearance kinetics, we tested the hypothesis that a three-parameter model that replaces Michaelis–Menten kinetics with first-order kinetics might fit some of our data. The parsimonious three-parameter model provides excellent fits to the lag, overshoot, and hang-up features of the postnomifensine responses in the fast and slow domains of the DS and NAc (Figure 6). The parameters (Table 2) indicate that after nomifensine treatment (1) DA release and uptake are faster in the DS and NAc fast domains compared to their respective slow domains and (2) the transport parameter is larger in the DS domains compared to that in the NAc domains. Given the excellent fit of the first-order model, great caution should be exercised in attempting to draw conclusions about V_{max} and K_M from simulations of responses recorded in nomifensine-treated animals: the responses in Figure 6 contain no information about V_{max} and K_M.

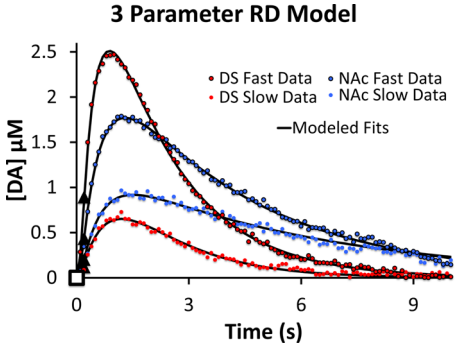

Figure 6. Three-parameter RD simulations of postnomifensine averaged responses to 0.2 s, 60 Hz stimuli recorded in the dorsal striatum and the nucleus accumbens. Parameter values are reported in Table 2.

Table 2. RD Simulation Parameters for Figure 6

	R_p (mols × 10^{-21})	k (s^{-1})	T (s^{-1})
DS fast, 0.2 s + nomi	25	2.54	0.51
DS slow, 0.2 s + nomi	3.7	1.30	0.59
NAc fast, 0.2 s + nomi	24	1.93	0.26
NAc slow, 0.2 s + nomi	17	1.84	0.17

CONCLUSIONS

The RD simulations successfully reproduce the lag, overshoot, and hang-up features of evoked responses recorded in the fast and slow domains of the DS and NAc over a range of stimulus conditions and in animals treated with nomifensine. Hence, the model mathematically validates the hypothesis that DA undergoes restricted diffusion in the extracellular space. However, the model does not prove that the restricted diffusion mechanism is correct, only that it is a plausible mechanism.

The major contribution of this work, therefore, is the demonstration of the existence and importance of T, a new parameter not previously mentioned in the DA modeling literature. Integrating eq 4 and inserting the result into eq 5 (see Methods section) yields

$$\frac{d[DA]_{oc}}{dt} = \frac{R_p f}{V_{oc}}(1 - e^{-Tt}) - \frac{V_{max}[DA]_{oc}}{[DA]_{oc} + K_M} \quad (2)$$

Note that if T were set to infinity (equivalent to instantaneous transport from the IC to the OC) then eq 2 would be equivalent to eq 1. Mathematically, T is a parameter that modulates the delivery of DA to the extracellular space. It is plausible that this modulation involves transport, as we have hypothesized, but we cannot exclude other possible mechanisms. Identifying the specific causes for the time-dependence of the parameters and fully realizing the implications of the new T parameter will undoubtedly require further investigation.

METHODS

Original Diffusion Gap (DG) Model. Compactly stated, the DG model is[16]

$$\frac{d[DA]}{dt} = D\frac{\partial^2[DA]}{\partial x^2} + [DA]_p f - \frac{V_{max}[DA]}{[DA] + K_M} \quad (3)$$

where the first term on the right is the planar diffusion operator, x and t are the coordinates of space and time, respectively, and the other terms were explained above (see eq 1). From the initial condition of $[DA]_{x,t=0} = 0$, eq 3 was solved for $[DA]_{x,t}$ by a finite element method (see Supporting Information for additional details and example code), with the diffusion gap (width = w_g) interposed between the electrode and a region of active DA release and uptake.[28] The five adjustable parameters are the concentration of dopamine released per stimulus pulse ($[DA]_p$), the maximal rate and Michaelis constant of DA uptake (V_{max} and K_M, respectively), DA's diffusion coefficient (D), and the width of the gap, w_g.

To reduce the number of adjustable parameters to four, we used a dimensionless gap parameter, $Gap = w_g/(D/60)^{1/2}$ (where 60 Hz was chosen as convenient time base for the simulations of interest here). We used this dimensionless parameter because there is no reason to retain D and w_g as independently adjustable parameters: rapid diffusion across a wide gap is equivalent to slow diffusion across a narrow gap and vice versa. With the D of DA in the striatum (2.4×10^{-6} cm^2 s^{-1}),[29] a Gap of 1 corresponds to a physical gap of 2 μm. With the D of DA in Nafion (1×10^{-9} cm^2 s^{-1}),[30] a Gap of 5 corresponds to a film thickness of 200 nm.

Restricted Diffusion (RD) Model. The new RD model comprises two coupled differential equations

$$\frac{dDA_{ic}}{dt} = R_p f - DA_{ic} T \quad (4)$$

$$\frac{d[DA]_{oc}}{dt} = \frac{DA_{ic} T}{V_{oc}} - \frac{V_{max}[DA]_{oc}}{[DA]_{oc} + K_M} \quad (5)$$

where DA_{ic} is the amount of DA (moles) trapped in the inner compartment, V_{oc} is the volume of the outer compartment, and $[DA]_{oc}$ is the concentration of DA in the outer compartment (other terms are defined similarly to the DG model). The new model has four adjustable parameters: R_p is the amount of DA (moles) released per stimulus pulse, T is a first-order reaction rate constant that describes the transport of DA from the inner to the outer compartment, and V_{max} and K_M are the Michaelis–Menten parameters for uptake from the OC.

The RD model describes the transport of DA from the inner to the outer compartment as if it were a chemical reaction. This is the same strategy used throughout the DA modeling literature to describe DA uptake, the mass transport of DA through a transmembrane passageway formed by the DAT, as a chemical reaction exhibiting Michaelis–Menten kinetics. We have assumed that transport from the inner to the outer compartment is a first-order event because, at

dx.doi.org/10.1021/cn5000666 | ACS Chem. Neurosci. 2014, 5, 776–783

present, there is nothing to suggest that the compartments exhibit DA affinity. It should be mentioned that this strategy for modeling transport involves a simplifying approximation because, in both cases, the model is cast as if the chemical reactions are irreversible.

As mentioned above, the RD model does not postulate that DA is taken up from the inner compartment. It might be the case that uptake is not active within the inner compartment. Alternately, it might be that uptake from the inner compartment prevents some DA from ever reaching the outer compartment, rendering a fraction of the released DA invisible to FSCV; in that case, the R_p value is an apparent value that represents the net amount of DA that exits the inner compartment, which might be less than the total amount released.

The RD simulations were implemented with a finite element method, again starting with the initial condition that the extracellular space contains no evoked DA (see Supporting Information for additional details and example code). Inspired by the ultrastructure of the striatum,[31] we fixed V_{oc} to 16 μm^3; it turns out that any value could be used with a corresponding adjustment of R_p, so there is no purpose to treating V_{oc} as an adjustable parameter.

Curve Fitting. We encountered the local minimum problem in our attempts to use Simplex optimization[35] for curve fitting. So, instead, we used a brute-force algorithm. Starting with an initial set of parameters, the algorithm evaluated the fit produced by 80 adjacent parameter sets (see Supporting Information for additional details), retained the set that produced the best fit (smallest sum of squared differentials), and repeated the process starting over with the retained best-fit parameters. The search was repeated until the algorithm could make no further improvement in the fit.

In Vivo Recordings. In this article, we compare simulated overflows to previously published overflows recorded in the DS and NAc. The detailed experimental procedures are also previously published.[18−20,32] Briefly, all of the recordings were performed with microelectrodes formed with single carbon fibers (diameter = 7 μm, length = 200 μm, T650 fibers, Cytec Carbon Fibers, Piedmont, SC) sealed into pulled borosilicate capillaries with low-viscosity epoxy (Spurr, Polysciences, Warrington, PA). Fast-scan cyclic voltammetry employed a triangular potential waveform (0 to 1 V to −0.5 to 0 V at 400 V s^{-1}) applied at a repetition rate of 10 Hz. The reference electrode was Ag/AgCl. The microelectrodes were calibrated after the in vivo experiments.

The University of Pittsburgh Institutional Animal Care and Use Committee approved all procedures involving animals. Male Sprague−Dawley rats (250−350 g, Hilltop, Scottsdale, PA) were anesthetized with isoflurane (2.5% by volume in O_2), wrapped in a 37 °C homeothermic blanket (Harvard Apparatus, Holliston, MA) and placed in a stereotaxic frame (Kopf, Tujunga, CA). A stainless steel, twisted bipolar stimulating electrode (MS303/a, Plastics One, Roanoke, VA) was placed into the medial forebrain bundle, and a carbon fiber microelectrode was placed either into the ipsilateral DS or NAc: detailed stereotaxic coordinates and procedures are published.[18−20,32] The MFB was stimulated with a biphasic, constant-current, square wave delivered by a stimulus isolator (Neurolog 800, Digitimer, Letchworth Garden City, UK). The responses analyzed during this work were all obtained with a stimulus frequency of 60 Hz, a current intensity of 250 μA, and pulse duration of 2 ms. The stimulus duration was variable and is specified in the Results and Discussion section.

The postnomifensine-evoked responses analyzed during this study were recorded 30 min after rats received a single dose of nomifensine (20 mg kg^{-1} i.p.).

■ ASSOCIATED CONTENT

Supporting Information

Parameter values, example code for DG and RD models, and details of the parameter search algorithm. This material is available free of charge via the Internet at http://pubs.acs.org.

■ AUTHOR INFORMATION

Corresponding Author

*E-mail: amichael@pitt.edu. Phone: 412-624-8560.

Author Contributions

Walters conceived of the model and fit it to the data. Taylor and Shu provided critical discussions of their in vivo observations of evoked DA release. Walters and Michael coauthored the manuscript. All authors reviewed and approved the manuscript.

Funding

This work was financially supported by the NIH (MH 075989, NS086107).

Notes

The authors declare no competing financial interest.

■ ABBREVIATIONS

DA, dopamine; DAT, dopamine transporter; FSCV, fast-scan cyclic voltammetry; DS, dorsal striatum; NAc, nucleus accumbens; IC, inner compartment; OC, outer compartment

■ REFERENCES

(1) Schultz, W. (2007) Multiple dopamine functions at different time courses. *Annu. Rev. Neurosci. 30*, 259−288.

(2) Abi-Dargham, A., Rodenhiser, J., Printz, D., Zea-Ponce, Y., Gil, R., Kegeles, L. S., et al. (2000) Increased baseline occupancy of D2 receptors by dopamine in schizophrenia. *Proc. Natl. Acad. Sci. U.S.A. 97*, 8104−8109.

(3) Schultz, W. (1982) Depletion of dopamine in the striatum as an experimental model of Parkinsonism: direct effects and adaptive mechanisms. *Prog. Neurobiol. (Oxford, U.K.) 18*, 121−166.

(4) Sagvolden, T., Johansen, E. B., Aase, H., and Russell, V. A. (2005) A dynamic developmental theory of attention-deficit/hyperactivity disorder (ADHD) predominantly hyperactive/impulsive and combined subtypes. *Behav. Brain Sci. 28*, 397−419.

(5) Carlsson, A., Lindqvist, M., Magnusson, T., and Waldeck, B. (1958) On the presence of 3-hydroxytyramine in brain. *Science 127*, 471.

(6) May, L. J., Kuhr, W. G., and Wightman, R. M. (1988) Differentiation of dopamine overflow and uptake processes in the extracellular fluid of the rat caudate nucleus with fast-scan in vivo voltammetry. *J. Neurochem. 51*, 1060−1069.

(7) Iversen, L. L. (1971) Role of transmitter uptake mechanisms in synaptic neurotransmission. *Br. J. Pharmacol. 41*, 571−591.

(8) Sharp, T., Zetterstrom, T., and Ungerstedt, U. (1986) An in vivo study of dopamine release and metabolism in rat brain regions using intracerebral dialysis. *J. Neurochem. 47*, 113−122.

(9) Nicholson, C. (1995) Interaction between diffusion and Michaelis−Menten uptake of dopamine after iontophoresis in striatum. *Biophys. J. 68*, 1699−1715.

(10) Rice, M. E., Oke, A. F., Bradberry, C. W., and Adams, R. N. (1985) Simultaneous voltammetric and chemical monitoring of dopamine release in situ. *Brain Res. 340*, 151−155.

(11) Keithley, R. B., Takmakov, P., Bucher, E. S., Belle, A. M., Owesson-White, C. A., Park, J., et al. (2011) Higher sensitivity dopamine measurements with faster-scan cyclic voltammetry. *Anal. Chem. 83*, 3563−3571.

(12) Owesson-White, C. A., Roitman, M. F., Sombers, L. A., Belle, A. M., Keithley, R. B., Peele, J. L., et al. (2012) Sources contributing to the average extracellular concentration of dopamine in the nucleus accumbens. *J. Neurochem. 121*, 252−262.

(13) Kile, B. M., Walsh, P. L., McElligott, Z. A., Bucher, E. S., Guillot, T. S., Salahpour, A., et al. (2012) Optimizing the temporal resolution of fast-scan cyclic voltammetry. *ACS Chem. Neurosci. 3*, 285−292.

(14) Ariansen, J. L., Heien, M. L., Hermans, A., Phillips, P. E., Hernadi, I., Bermudez, M. A., et al. (2012) Monitoring extracellular

pH, oxygen, and dopamine during reward delivery in the striatum of primates. *Front. Behav. Neurosci. 6*, 36.
(15) Garris, P. A., Budygin, E. A., Phillips, P. E., Venton, B. J., Robinson, D. L., Bergstrom, B. P., et al. (2003) A role for presynaptic mechanisms in the actions of nomifensine and haloperidol. *Neuroscience 118*, 819−829.
(16) Wightman, R. M., Amatore, C., Engstrom, R. C., Hale, P. D., Kristensen, E. W., Kuhr, W. G., et al. (1988) Real-time characterization of dopamine overflow and uptake in the rat striatum. *Neuroscience 25*, 513−523.
(17) Kawagoe, K. T., Garris, P. A., Wiedemann, D. J., and Wightman, R. M. (1992) Regulation of transient dopamine concentration gradients in the microenvironment surrounding nerve terminals in the rat striatum. *Neuroscience 51*, 55−64.
(18) Taylor, I. M., Jaquins-Gerstl, A., Sesack, S. R., and Michael, A. C. (2012) Domain-dependent effects of DAT inhibition in the rat dorsal striatum. *J. Neurochem. 122*, 283−294.
(19) Taylor, I. M., Ilitchev, A. I., and Michael, A. C. (2013) Restricted diffusion of dopamine in the rat dorsal striatum. *ACS Chem. Neurosci. 4*, 870−878.
(20) Shu, Z., Taylor, I. M., and Michael, A. C. (2013) The dopamine patchwork of the rat nucleus accumbens core. *Eur. J. Neurosci. 38*, 3221−3229.
(21) Moquin, K. F., and Michael, A. C. (2009) Tonic autoinhibition contributes to the heterogeneity of evoked dopamine release in the rat striatum. *J. Neurochem. 110*, 1491−1501.
(22) Wang, Y., Moquin, K. F., and Michael, A. C. (2010) Evidence for coupling between steady-state and dynamic extracellular dopamine concentrations in the rat striatum. *J. Neurochem. 114*, 150−159.
(23) Moquin, K. F., and Michael, A. C. (2011) An inverse correlation between the apparent rate of dopamine clearance and tonic autoinhibition in subdomains of the rat striatum: a possible role of transporter-mediated dopamine efflux. *J. Neurochem. 117*, 133−142.
(24) Hrabetova, S., and Nicholson, C. (2004) Contribution of dead-space microdomains to tortuosity of brain extracellular space. *Neurochem. Int. 45*, 467−477.
(25) Ogston, A. G., Preston, B. N., and Wells, J. D. (1973) On the transport of compact particles through solutions of chain-polymers. *Proc. R. Soc. London, Ser. A 333*, 297−316.
(26) Johnson, E. M., Berk, D. A., Jain, R. K., and Deen, W. M. (1996) Hindered diffusion in agarose gels: test of effective medium model. *Biophys. J. 70*, 1017−1023.
(27) Hrabetova, S., Masri, D., Tao, L., Xiao, F., and Nicholson, C. (2009) Calcium diffusion enhanced after cleavage of negatively charged components of brain extracellular matrix by chondroitinase ABC. *J. Physiol. 587*, 4029−4049.
(28) Venton, B. J., Zhang, H., Garris, P. A., Phillips, P. E., Sulzer, D., and Wightman, R. M. (2003) Real-time decoding of dopamine concentration changes in the caudate-putamen during tonic and phasic firing. *J. Neurochem. 87*, 1284−1295.
(29) Nicholson, C, and Rice, M. E. (1991) Diffusion of ions and transmitters in the brain cell microenvironment. In *Volume Transmission in the Brain* (Fuxe, K., and Agnati, L. F., Eds.) pp 279−294, Raven Press, New York.
(30) Kristensen, E. W., Kuhr, W. G., and Wightman, R. M. (1987) Temporal characterization of perfluorinated ion exchange coated microvoltammetric electrodes for in vivo use. *Anal. Chem. 59*, 1752−1757.
(31) Moss, J., and Bolam, J. P. (2008) A dopaminergic axon lattice in the striatum and its relationship with cortical and thalamic terminals. *J. Neurosci. 28*, 11221−11230.
(32) Shu, Z., Taylor, I. M., Walters, S. H., and Michael, A. C. (2014) Region- and domain-dependent action of nomifensine. *Eur. J. Neurosci.*, DOI: 10.1111/ejn.12604, published online Apr 26.
(33) Stamford, J. A., Kruk, Z. L., Palij, P., and Millar, J. (1988) Diffusion and uptake of dopamine in rat caudate and nucleus accumbens compared using fast cyclic voltammetry. *Brain Res. 448*, 381−385.
(34) Cass, W. A., Gerhardt, G. A., Mayfield, R. D., Curella, P., and Zahniser, N. R. (1992) Differences in dopamine clearance and diffusion in rat striatum and nucleus accumbens following systemic cocaine administration. *J. Neurochem. 59*, 259−266.
(35) Wu, Q., Reith, M. E., Wightman, R. M., Kawagoe, K. T., and Garris, P. A. (2001) Determination of release and uptake parameters from electrically evoked dopamine dynamics measured by real-time voltammetry. *J. Neurosci. Methods 112*, 119−133.
(36) Engstrom, R. C., Wightman, R. M., and Kristensen, E. W. (1988) Diffusional distortion in the monitoring of dynamic events. *Anal. Chem. 60*, 652−656.
(37) Heien, M. L., Johnson, M. A., and Wightman, R. M. (2004) Resolving neurotransmitters detected by fast-scan cyclic voltammetry. *Anal. Chem. 76*, 5697−5704.
(38) Bath, B. D., Michael, D. J., Trafton, B. J., Joseph, J. D., Runnels, P. L., and Wightman, R. M. (2000) Subsecond adsorption and desorption of dopamine at carbon-fiber microelectrodes. *Anal. Chem. 72*, 5994−6002.
(39) Near, J. A., Bigelow, J. C., and Wightman, R. M. (1988) Comparison of uptake of dopamine in rat striatal chopped tissue and synaptosomes. *J. Pharm. Exp. Ther. 245*, 921−927.
(40) Wu, Q., Reith, M. E., Kuhar, M. J., Carroll, F. I., and Garris, P. A. (2001) Preferential increases in nucleus accumbens dopamine after systemic cocaine administration are caused by unique characteristics of dopamine neurotransmission. *J. Neurosci. 21*, 6338−6347.
(41) Einhorn, L. C., Johansen, P. A., and White, F. J. (1988) Electrophysiological effects of cocaine in the mesoaccumbens dopamine system: studies in the ventral tegmental area. *J. Neurosci. 8*, 100−112.
(42) Wu, Q., Reith, M. E., Walker, Q. D., Kuhn, C. M., Carroll, F. I., and Garris, P. A. (2002) Concurrent autoreceptor-mediated control of dopamine release and uptake during neurotransmission: an in vivo voltammetric study. *J. Neurosci. 22*, 6272−6281.